Hybrid Advances 6 (2024) 100201

Contents lists available at ScienceDirect

Hybrid Advances

journal homepage: www.journals.elsevier.com/hybrid-advances

Poly(acid lactic)-montmorillonite clay bionanocomposites loaded with tea tree oil for application in antibacterial wound healing

Larissa Braga Proença [a], Gabriela Marinho Righetto [b], Ilana Lopes Baratella da Cunha Camargo [b], Marcia Cristina Branciforti [a,*]

[a] Department of Materials Engineering, School of Engineering of Sao Carlos, University of Sao Paulo. Avenida Trabalhador Sao-carlense, 400, Sao Carlos, CEP 13566-590, Brazil

[b] Sao Carlos Institute of Physics, University of Sao Paulo. Avenida Trabalhador Sao-carlense, 400, Sao Carlos, CEP 13566-590, Brazil

ARTICLE INFO

Keywords:
Montmorillonite clay
Tea tree essential oil
Antibacterial
Dressing
Bionanocomposite
poly(acid lactic)

ABSTRACT

This study evaluated the ability of tea tree essential oil (TT) incorporated into polymer-clay bionanocomposites to *in vitro* eliminate resistant microorganisms towards applications in antibacterial wound healing. Antimicrobial bionanocomposites were prepared in two steps, namely sonication and melt intercalation, and montmorillonite clay and poly(acid lactic) (PLA) were chosen because they constitute a polymer-clay bionanocomposite to be applied in wound dressing. X-ray diffraction (XRD) results indicated good incorporation of the organic compounds, TT oil, and glycerol (G) (the latter used as a plasticizer) into the clay galleries. Dynamic-mechanical analysis (DMA) results showed a 2–30 % increase in storage modulus and up to 10 °C decrease in glass transition temperature, proving the influence of both TT oil and G on the stress transfer of the reinforcement clay phase. Thermogravitmetric analyses (TGA) revealed TT oil and G addition worsened the thermal stability of the bionanocomposites, which show a mass loss onset decrease up to 90 °C and a clay content between 1.5 and 3 wt %. *In vitro* antimicrobial activity tests revealed only the combinations of TT oil and G reduced *Escherichia coli* and *Staphylococcus aureus* satisfactorily and showed the antimicrobial activity of the bionanocomposites.

1. Introduction

Biopolymers are materials obtained from natural sources such as corn, sugarcane, maize, potate, and others, and, therefore, can potentially replace polymers derived from fossil sources, being attractive for sustainable production [1]. They can be used as vehicles of incorporating additives, such as antioxidants, antimicrobial, and antifungal agents [2]. Their important properties include biodegradability and biocompatibility. All such features have enabled their use in drug delivery systems for health care and tissue engineering applications [3]. Poly(acid lactic) (PLA) is one of the most used synthetic polymers for the production of wound dressing [1,4] and also bio-based active packaging [5], since it is a biocompatible and biodegradable material with good mechanical durability and elasticity. Besides, PLA is US Food and Drug Administration approved for a wide range of biomedical applications such as wound dressing. The production of PLA has multiple advantages, including the lactide monomer produced from lactic acid, which is obtained from the fermentation of renewable resources like sugarcane, and corn, it reduces the wastes disposed of in landfills and it saves energy, in addition PLA has good physical properties and, its modifications can optimize its properties to a certain extent [5].

The direct incorporation of antimicrobial agents into polymers causes a rapid depletion of the active compound, implying a short antimicrobial effect [6]. An alternative is to produce bionanocomposites based on biopolymers matrices and reinforcement nanoparticles [7]. Montmorillonite is a nanoclay commonly used in biopolymers. Melt intercalation is the most applied method for bionanocomposite production because it is simple and enables continuous and large-scale production [8]. It consists of heating the polymer and clay mixture at a temperature above the polymer's melting point and keeping it under shear for the intercalation or exfoliation of the nanoparticles [2]. Some studies have shown that adding glycerol during the mixing process can improve the polymer matrix's exfoliation results and the clay dispersion level [9]. The main advantage of montmorillonite for applications in drug delivery systems is related to the lamellar structure of the clay, which, combined with polymers, improves the barrier properties of the

* Corresponding author.
E-mail address: marciacb@sc.usp.br (M.C. Branciforti).

https://doi.org/10.1016/j.hybadv.2024.100201
Received 19 January 2024; Received in revised form 11 April 2024; Accepted 18 April 2024
Available online 20 April 2024

bionanocomposite, promoting a controlled release of bioactive molecules [6,10].

Different types of drugs (e.g., chemotherapeutic agents, antivirals, antimicrobials, anti-inflammatories), hormones, and antigens can be applied in controlled release systems. Herbal medicines can also be used due to their antimicrobial and antifungal properties [11]. Tea tree essential oil (TT), for example, has antibacterial, antiviral, and anti-inflammatory properties and is efficient against gram-positive and gram-negative bacteria. Therefore, it can be used in the treatment of infectious diseases, food preservation, and as potential sources of new antimicrobial compounds [12–15].

The essential oil can be introduced to nanoparticles through nanoemulsion systems. Due to the limitations of essential oils in commercial applications, i.e., low water solubility, emulsifiers, such as Tween 80, have been used to overcome this problem of solubility [7,16,17].

The combination of nanoclay and essential oil into biopolymers has resulted in materials of improved mechanical and thermal properties and excellent antibacterial and antioxidant activities [7,18]. Therefore, it was chose PLA, montmorillonite clay, tea tree (TT) essential oil, and glycerol for constituting bionanocomposites for *in vitro* evaluation for possible application in antibacterial wound dressing. The studied system has multiple benefits, including the lamellar structure of the clay, that combined with the biopolymer, improves barrier properties and promots controlled release of antibacterial, antiviral, and anti-inflammatory molecules of TT essential oil of the wound dressing; another benefit is related to the PLA similarity to macromolecules recognized by the human body.

The paper show how it was incorporated TT essential oil into montmorillonite, obtained the bionanocomposites, evaluated the effective incorporation of montmorillonite into the clay lamellas, the extent of clay intercalation/exfoliation, the bionanocomposite morphology, thermo-mechanical and thermal properties of the bionanocomposites. Finally, the bionanocomposites *in vitro* analyzed against gram-positive and gram-negative bacteria and accessed the influence of TT oil and glycerol on clay exfoliation and mechanical, thermal, and morphologic behaviors.

2. Experimental details

2.1. Materials

An extrusion grade of PLA, Ingeo™ Biopolymer 2003D, from Nature Works, USA, of 210 °C melting temperature, 24 g cm^{-3} density, and 6 g 10 min^{-1} (210 °C and 2.16 kg) melt flow index was chosen as the bionanocomposite matrix. Nanoclay (Clay) was an organically modified montmorillonite, Cloisite® 20A, from Southern Clay Products Inc., USA, and tea tree (TT) essential oil was purchased from Amazon, Brazil. Glycerol (G), used as a plasticizer, and Tween 80, used as a non-ionic emulsifier, were purchased from Sigma-Aldrich, Brazil.

2.2. Incorporation of tea tree oil into montmorillonite clay

Samples with different compositions were prepared by mixing a constant ratio of montmorillonite clay and G and different rations (0.1 and 0.2) of TT essential oil. Tween 80 was added in the 0.25g/1g proportion to TT essential oil. First, each mixture was dispersed in 50 mL of deionized water and stirred for 1 min by an Ultra-Turrax T25 (IKA Labortechnik) at 19,000 rpm in a closed bottle and ice bath. The suspension sonication was performed by a 400W power Hielscher UP400S tip ultrasonicator, at 20 KHz frequency for 30 min, while the suspension was in a bottle in an ice bath, and covered by a lid, which had a hole in the middle. Finally, the samples were dried in a vacuum oven for 24 h. These samples are named ultrasonicated samples and are abbreviated as Clay/G, Clay/10TT, Clay/10 TT/G, Clay/20TT, and Clay/20 TT/G (Table 1).

Table 1
2θ angle values of nanoclay's main diffraction peak and interlamellar distance, $d_{(001)}$, of pure clay and ultrasonicated and extruded bionanocomposites samples.

Sample	2θ (°)	$d_{(001)}$ (nm)	Sample	2θ (°)	$d_{(001)}$ (nm)
Clay	3.50	2.55 ± 0.05	PLA/Clay	2.50	3.53 ± 0.05
Clay/G	2.80	3.15 ± 0.05	PLA/Clay/G	2.36	3.74 ± 0.05
Clay/10TT	2.50	3.53 ± 0.05	PLA/Clay/10TT	2.26	3.91 ± 0.05
Clay/10 TT/G	2.10	4.20 ± 0.05	PLA/Clay/10 TT/G	2.34	3.77 ± 0.05
Clay/20TT	2.20	4.01 ± 0.05	PLA/Clay/20TT	2.24	3.94 ± 0.05
Clay/20 TT/G	2.10	4.20 ± 0.05	PLA/Clay/20 TT/G	2.26	3.91 ± 0.05

2.3. Preparation of bionanocomposites

Bionanocomposite of PLA with 3 wt% of clay was prepared, and bionanocomposites of PLA with each ultrasonicated sample were prepared, all with a final composition of 3 wt% of clay. All bionanocomposites were melt compounded by a single screw (D = 16 mm and L/D = 26) AX Plastics extruder of 30 rpm screw speed and temperature profiles of 185, 190, and 190 °C, to feed, compression, and dosing zones, respectively. The extruder die output time was optimized to collect the first portion of material, since the material is not homogeneous from the beginning. The resulting pellets were thermo-pressed at 180 °C, under 150 bar, and cooled at room temperature for obtaining the bionanocomposite films of approximately 1.2 ± 0.1 mm thickness. These samples are named bionanocomposites samples and are abbreviated as PLA/Clay/G, PLA/Clay/10TT, PLA/Clay/10 TT/G, PLA/Clay/20TT, and PLA/Clay/20 TT/G (Table 1).

2.4. X-ray diffraction (XRD) analyses

XRD analyses were conducted on a Rigaku Ultima IV diffractometer using a sealed Cu tube ($\lambda_{Cu-k\alpha} = 1.5405$ Å) of 1° min^{-1} scanning speed in a 1.5–40° 2θ range at 0.02° s^{-1} steps and 40 kV and 40 A. The interlamellar distance of (001) peak was calculated by Bragg's Law, Equation (1) [19].

$$n\,\lambda = 2\,d_{(001)}\,sin\,\theta \quad (1)$$

where n is diffraction number 1, λ is the radiation wavelength, $d_{(001)}$ is the interlamellar distance in nm, and θ is the diffraction angle measured.

2.5. Dynamic-mechanical analyses (DMA)

A dynamic-mechanical analyses conducted in PerkinElmer DMA 8000 equipment evaluated the effect of clay on the thermo-mechanical properties of the bionanocomposite. Tests were performed in a traction module with samples of 50 x 10 × 1 mm, under uncontrolled atmosphere, at 3 °C min^{-1} heating rate,1 Hz frequency, and 25–150 °C temperature range.

2.6. Thermogravimetric analyses (TGA)

Thermogravimetric analyses were performed on PerkinElmer Pyris 1 TGA equipment under an inert atmosphere of nitrogen gas (20 mL min^{-1}), heating the samples from 25 °C to 300 °C for TT oil and 600 °C for the other samples, at 20 °C min^{-1} heating rate.

2.7. Evaluation of antimicrobial activity of the plastic surface with bionanocomposites

Bionanocomposite films were produced for accessing their

antimicrobial activity against *Staphylococcus aureus* ATCC 25923 and *Escherichia coli* ATCC25922, based on the ISO221961 standard method with slight modifications. For this study, it used 40 mm square and 1 mm thick test specimens, 32 mm square and 1 mm thick polypropylene cover films, and 256 µl bacterial inoculum at 6×10^5 CFU mL^{-1}. It was tested specimens containing PLA, PLA/Clay, PLA/Clay/10TT, PLA/Clay/10 TT/G, PLA/Clay/20TT, and PLA/Clay/20 TT/G, using neat PLA as the control group.

Both cover films were cleaned, and test specimens with 70 % alcohol solution before inoculating the bacteria. The Petri dishes, containing the inoculated test specimens covered with polypropylene cover film at 35 ± 1 °C for 24h, were incubated. The bacteria were recovered of a replicate of the specimen test prepared as described immediately after the inoculation to calculate the average of the common logarithm of the number of viable bacteria, in CFU cm^{-2} (U0). It was calculated the number of viable cells on each bionanocomposite specimen after mixing 10 mL of soybean casein lecithin polysorbate 80 (SCDLP) media, serially diluting it on phosphate-buffered physiological saline, and cultivating 900 µL on count agar at 35 ± 1 °C for 48h.

It was accessed conditions for a valid test, according to ISO 221961, and observed 1) the difference in the logarithmic value of the maximum and minimum numbers of viable bacteria divided by the mean value of viable bacteria recovered immediately after inoculation from the untreated test specimens (L) should be ≤ 0.2; 2) the average number of viable bacteria recovered immediately after inoculation from the untreated test specimens (N) should range between 6.2×10^3 CFU cm^{-2} and 2.5×10^4 CFU cm^{-2}; and 3) the number of viable bacteria recovered from each untreated test specimen after incubation for 24 h (N24) should not be lower than 6.2×10^1 CFU cm^{-2}.

It was calculated antimicrobial activity (R) as $U_t - A_t$, where U_t is the average of the common logarithm of the number of viable bacteria in CFU/cm^2 recovered from the untreated test specimens after 24 h, and A_t is the average of the common logarithm of the number of viable bacteria in CFU cm^{-2} recovered from the treated test specimens after 24 h. It was assessed whether there was a significant difference in CFU cm^{-2} among the untreated and treated specimens by ANOVA test.

3. Results and discussions

3.1. X-ray diffraction (XRD) analyses of ultrasonicated samples

It was evaluated the TT oil and glycerol incorporation into clay lamellas by XRD. Fig. 1 displays the X-ray diffractograms of the ultrasonicated samples, and Table 1 shows the 2θ angle values of nanoclay's main diffraction peak and the value of the interlamellar distance, $d_{(001)}$, calculated by Equation (1), of the samples subjected to ultrasound. Pure clay displayed the main diffraction peak at 2θ = 3.50°, which corresponds to an interlamellar distance, $d_{(001)}$, of 2.55 nm due to the organophilization process, in which Na^+ ions are replaced with long quaternary ammonium chains. Such values are consistent with those reported by Southern Clay Products Inc. and other authors [20,21]. Several studies [7,9,18] have shown that clays are capable to receive organic molecules between their lamellae and can be evaluated by their increased interlayer distance. When the organic compounds (TT oil and G) were mixed with clay, it was observed a substantial displacement of 2θ angle of nanoclay's main diffraction peak to lower value, indicating an increase in the interlamellar distances caused by the incorporation of TT oil and G into the clay galleries.

Ultrasonicated samples with only TT oil in different amounts, i.e., Clay/10TT and Clay/20TT samples, provided better intercalation results than samples with only G (Clay/G) - the higher the TT oil proportion, the higher the intercalation. The mixtures with both organic compounds (TT oil and G) resulted in a higher intercalation degree, as displayed in the Clay/10 TT/G and Clay/20 TT/G samples, which showed no difference in the degree of intercalation, despite the different amounts of TT oil, suggesting the maximum degree of intercalation was achieved for the studied compositions. However, the literature lacks studies of essential oil saturation between the nanoclay layers. Visually, the ultrasonicated samples were not necessarily homogeneous, than the DRX measurements were qualitatively and not quantitatively analized. According to the XRD results, the combination of TT oil and G, and the sonication method seem interesting for better clay/oil interaction results.

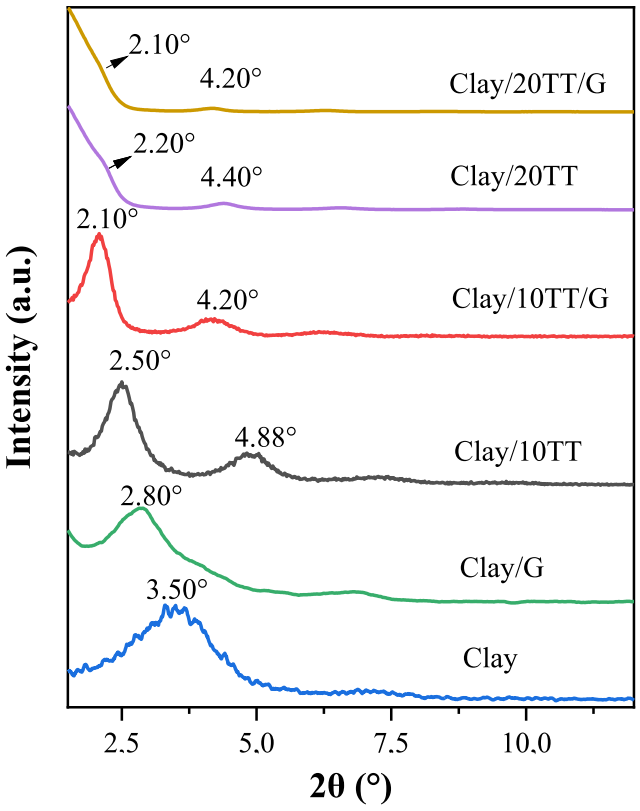

Fig. 1. X-ray diffractograms of pure clay, Clay/G, Clay/10TT, Clay/10 TT/G, Clay/20TT, and Clay/20 TT/G ultrasonicated samples.

3.2. X-ray diffraction (XRD) analyses of the bionanocomposites

After extrusion and thermo-pressing steps, the bionanocomposites were analyzed by XRD regarding the clay intercalation/exfoliation in the polymer matrix. Fig. 2 depicts the X-ray diffractograms of the extruded bionanocomposites, and Table 1 shows values of 2θ angle of nanoclay's main diffraction peak and the calculated value of the interlamellar distance, $d_{(001)}$.

PLA/Clay sample diffractogram revealed a shift of the clay $d_{(001)}$ peak from 2θ = 3.50° to 2θ = 2.50° (Table 1), hence, an increase in the basal spacing of the clay from 2.55 nm to 3.53 nm, indicating the penetration of PLA chains into clay interlamellar space. This result suggests that the processing steps promoted the formation of an intercalated structure of the PLA/Clay bionanocomposite. Regarding the composition of bionanocomposites, the PLA/Clay/G diffractogram shows G promoted a further shift of the clay peak to a lower value of 2θ = 2.36°, associated with a 3.74 nm interlamellar distance, thus indicating its action as a plastisizer favoring the formation of an even more intercalated structure when compared to the sample with no G. Visentini et al. [22] also observed that G addition decreases agglomeration and increases the intercalation of clay into the polymer matrix during the mixing process.

A synergistic effect occurs when TT oil is added to the mixture because the interplanar distance of (001) diffraction peak are further increased, as shown by the diffractograms of PLA/Clay/10TT, PLA/

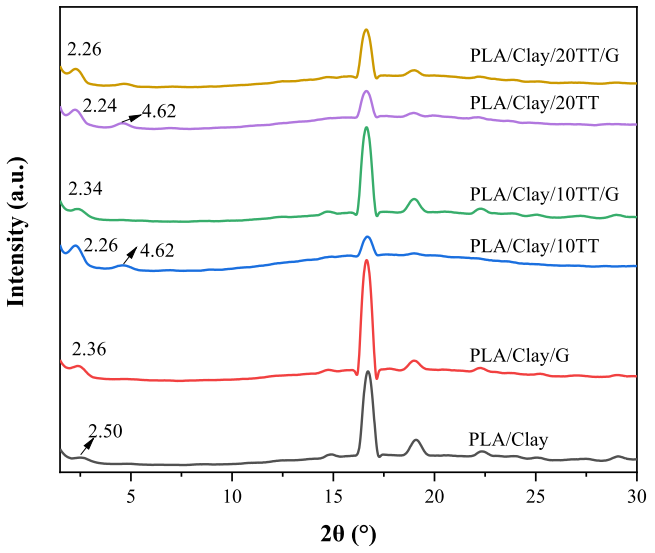

Fig. 2. X-ray diffractograms of PLA/Clay, PLA/Clay/G, PLA/Clay/10TT, PLA/Clay/10 TT/G, PLA/Clay/20TT, and PLA/Clay/20 TT/G extruded bionanocomposites.

Clay/20TT, PLA/Clay/10 TT/G, and PLA/Clay/20 TT/G bionanocomposites (Fig. 2). Most probably, the effective interaction between clay lamellae and the oil promotes the swelling of the nanofiller stacks, increasing the clay dispersion within the polymer matrix. As described by Zhu et al. [9] and Visentini et al. [22], essential oils can act as plasticizers, increasing chain mobility by weakening the intermolecular interactions and promoting the penetration of polymer chains into clay interlamellar space.

PLA/Clay/20TT and PLA/Clay/20 TT/G bionanocomposites (Fig. 2) showed a $d_{(001)}$ of 3.94 and 3.91 nm, respectively, suggesting no significant difference between the interactions of the samples without and with glycerol. However, the diffractogram of PLA/Clay/10 TT/G shows a slight widening and decrease of the $d_{(001)}$ peak intensity, indicating a partially exfoliated morphology of the bionanocomposite [23,24], probably favored by the presence of glycerol in the samples. Beauvalet et al. [25] observed an improvement in the clay dispersion when adding G to PLA montmorillonite clay nanocomposites. The XRD results show the nanoclay is in a mainly intercalated configuration in the bionanocomposites, which is in line with the literature a polymer nanocomposite usually exhibits an intercalated or intercalated/exfoliated nanostructure.

The XRD results can corroborate the transmission electron microscopy images, previously published [15], because such bionanocomposites can exhibit combined morphologies (e.g., intercalated-tactoid and intercalated-exfoliated). Furthermore, due to the impermeability of the clay layers, the exfoliated morphology increases the effect of tortuosity, promoting a controlled release of TT essential oil diffusion, which is extremely interesting in wound dressing application [18].

3.3. Dynamic-mechanical analyses (DMA)

DMA analyses were used to measure the glass transition temperature (Tg) and to evaluate the storage modulus (E′) of neat PLA and bionanocomposite films. Fig. 3 (a)-(b) displays the storage modulus (E′) and tan δ curves as a function of temperature, respectively, of neat PLA and bionanocomposite films. Table 2 shows the storage modulus of the samples at 25 °C with the percentage of gain and loss of E' in comparison to neat PLA, and the glass transition temperature, given by the first maximum of the tan δ peak in Fig. 3(b), of neat PLA and bionanocomposites.

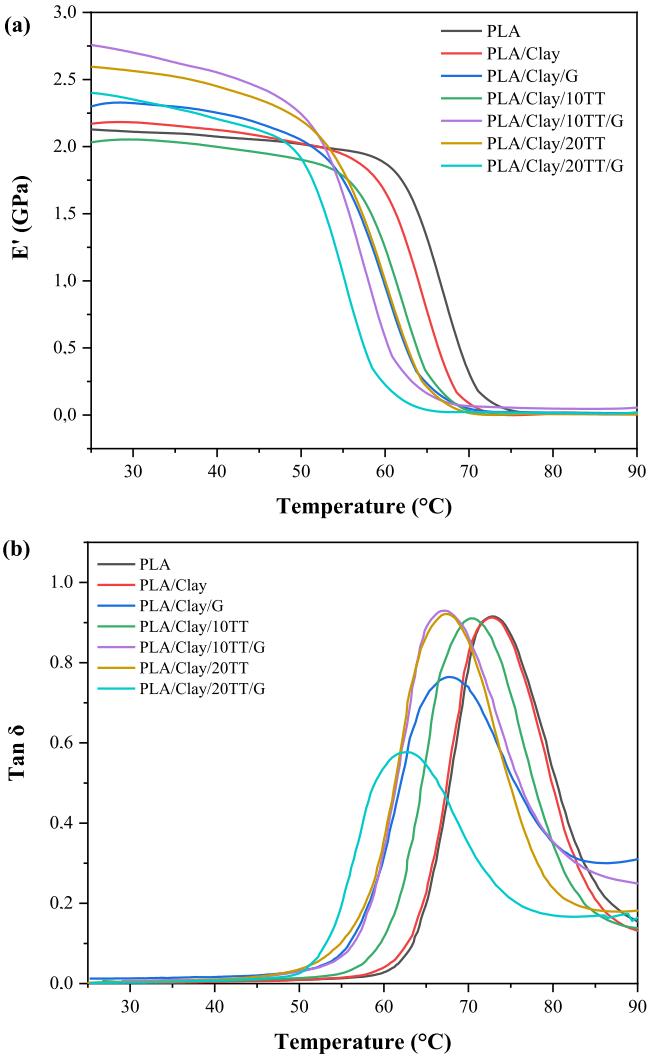

Fig. 3. (a) Storage modulus (E′) and (b) tan δ of neat PLA, PLA/Clay, PLA/Clay/G, PLA/Clay/10TT, PLA/Clay/10 TT/G, PLA/Clay/20TT, and PLA/Clay/20 TT/G extruded bionanocomposite films.

Table 2
Storage modulus (E′) and tan δ of PLA and bionanocomposites. The results in the brackets indicate an increase (+) or decrease (−) of E' in comparison to the neat PLA.

Sample	E' (GPa) at 25°C	tan δ (°C)
PLA	2.1	72.77
PLA/Clay	2.2 (+2 %)	72.69
PLA/Clay/G	2.3 (+8 %)	67.72
PLA/Clay/10TT	2.0 (-5 %)	70.24
PLA/Clay/10 TT/G	2.8 (+30 %)	67.24
PLA/Clay/20TT	2.6 (+22 %)	67.21
PLA/Clay/20 TT/G	2.4 (+13 %)	62.70

The E′ curves, shown in Fig. 3 (a), revealed that when adding clay to PLA (PLA/Clay sample), the modulus increased 2 % (Table 2) in comparison to the neat PLA, proving the influence of clay on the reinforcement in the viscoelastic state of the polymer. The other bionanocomposites also showed an increase in E′, between 8 and 30 %, except PLA/Clay/10TT, which showed a - 5 % decrease in the storage modulus, probably due to poor clay dispersion.

According to Fig. 3 (b), all samples showed 63–73 °C glass transition

temperature (Tg) given by the tan δ peak maximum. The comparison between PLA/Clay bionanocomposite and neat PLA revealed that the clay presence did not change the Tg of the sample and did not interfere with the relaxation of the PLA amorphous phase. On the other hand, in samples with both TT oil and G, the relaxation tan δ peaks shifted to lower temperatures. The reduction in Tg was found to be of the order of 10 °C for the PLA/Clay/20 TT/G nanocomposite. This reduction in Tg was expected because TT and G components act as plasticizers in the bionanocomposites, increasing the mobility of the polymer chains.

However, the E′ and tan δ curves showed no signicant differences in the viscoelastic state properties, indicating that the observed discrepancies in glassy state are primarily attributed to sample preparation and measurement errors.

3.4. Thermogravimetric analyses (TGA)

It was evaluated the thermal stability of the produced bionanocomposites by thermogravimetric analyses. Fig. 4(a)-(b) shows the TG and DTG curves, respectively, of TT essential oil, PLA, and the bionanocomposites. The clay (Cloisite® 20A) TGA analysis was previously published [21]. Table 3 shows the temperature of mass loss onset (T_{onset}), the maximum mass loss rate temperature (T_{max}), and the residual mass at 550 °C of TT essential oil, PLA, and the bionanocomposites studied.

The TT essential oil curve shows it is highly volatile even at lower temperatures, according to the literature observed [12–14]. Mass loss occurs in the 35–120 °C temperature range; the DTG curve (Fig. 4(b)) shows two maximum stages of mass loss - one at 77.20 °C and another at

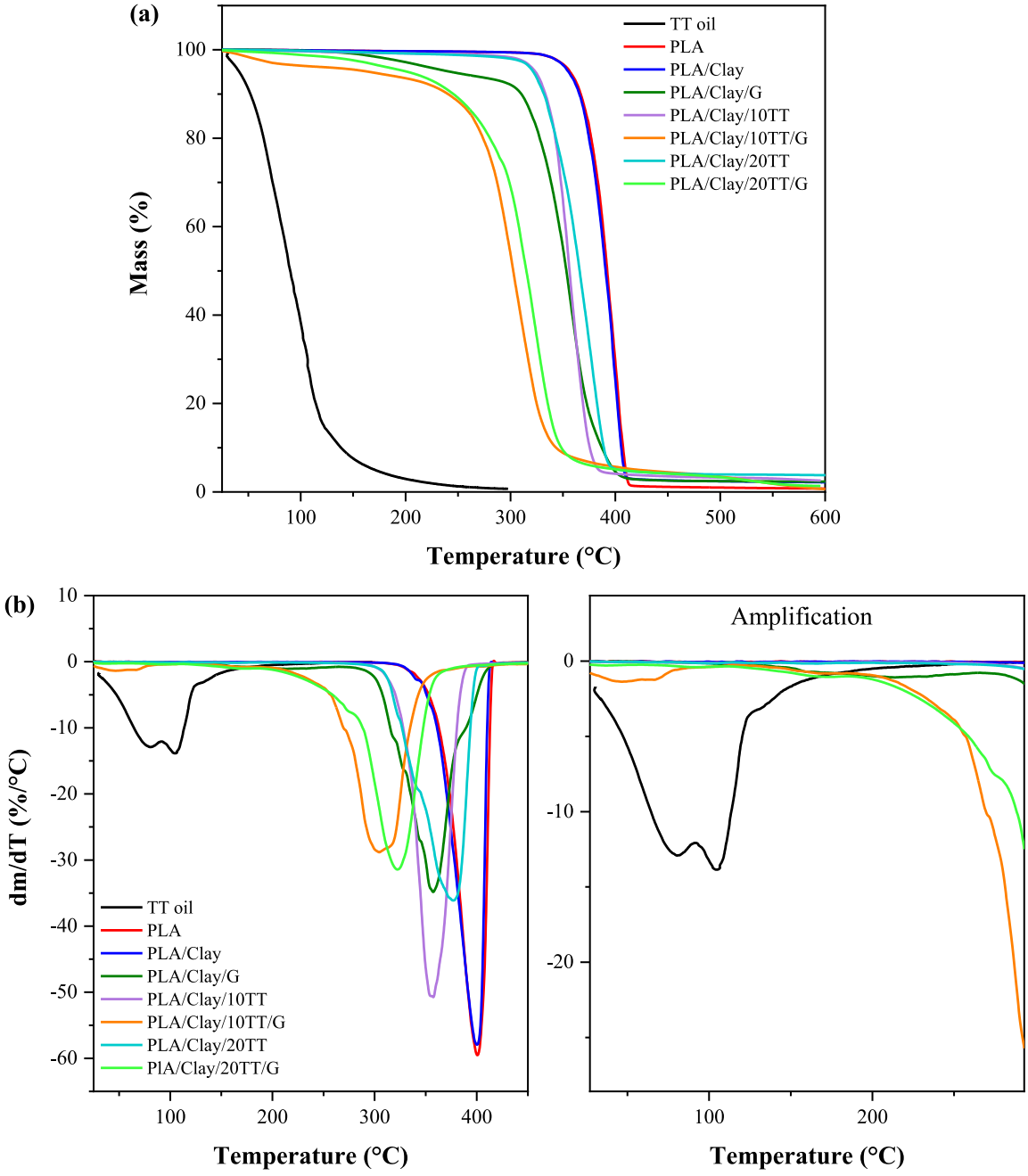

Fig. 4. (a) TG and (b) DTG curves of TT essential oil, PLA, PLA/Clay, PLA/Clay/G, PLA/Clay/10TT, PLA/Clay/10 TT/G, PLA/Clay/20TT, and PLA/Clay/20 TT/G extruded bionanocomposites.

Table 3
Temperature of mass loss onset (T_{onset}), temperature of maximum mass loss rate (T_{max}), and the residual mass percentage of TT oil, PLA, and bionanocomposites.

Sample	T_{onset}(°C)	T_{max} (°C)	Residue (%)
TT oil	35.00/55.94	77.20/105.79	0.72 (at 300 °C)
PLA	369.96	401.03	0.86
PLA/Clay	369.70	400.16	2.29
PLA/Clay/G	320.54	358.12	2.38
PLA/Clay/10TT	335.29	356.51	3.04
PLA/Clay/10 TT/G	35.00/133.00	50.00/304.35	1.87
PLA/Clay/20TT	338.80	376.76	3.90
PLA/Clay/20 TT/G	133.00	322.34	1.89

105.79 °C, both related to the volatility of the oil components. PLA sample show a maximum stage mass loss at 370 °C, referring to the PLA thermal degradation. PLA/Clay sample showed a single maximum stage mass loss at 370 °C, indicating that the clay addition did not cause any alteration in the thermal stability of the PLA/Clay bionanocomposite. The pure clay shows a main mass loss between 232 and 450 °C, atributted mainly to organic surfactant degradation [21]. Although the literature reports that clay incorporation improves the thermal stability of the nanocomposite, some studies have provided different results. Molinaro et al. [23] explained that the thermal degradation of nanocomposite might decrease at higher temperatures due to the lower stability of the clay organic modifier, and Paul et al. [28] claimed the low percentage of clay in the polymer matrix favors the intercalation/exfoliation. However, it is not enough to improve the thermal stability of the nanocomposite. PLA/Clay/G TGA result shows that the G addition reduces the thermal stability of the bionanocomposite by ~50 °C.

Nanocomposite samples with only TT essential oil, i.e., PLA/Clay/10TT and PLA/Clay/20TT, showed that the oil decreases the thermal stability of bionanocomposites. The mass loss onset temperatures decreased ~34 °C and 31 °C in PLA/Clay/10TT and PLA/Clay/20TT, respectively. The bionanocomposites with G, i.e., PLA/Clay/G, PLA/Clay/10 TT/G, and PLA/Clay/20 TT/G showed a stage of weight loss at ~133 °C, referring to the beginning of G and emulsifier evaporation, and another stage at ~304 °C, which is related to G and PLA thermal decomposition [28]. PLA/Clay/10 TT/G bionanocomposite showed an approximately 3 % mass reduction below 100 °C, probably related mostly to the volatilization of excess TT oil not necessarily incorporated in clay. Despite the high volatility of the essential oil, according to Giannakas et al. [29] the clay used as a carrier of active compounds can protect volatile molecules during processing steps. Additionally, as discussed above, the G addition reduces the thermal stability of the bionanocomposite by ~50 °C, consequently the samples with G addition show significant weight loss around processing temperature.

Finally, the thermograms also enabled analyses of the clay content and of the essential oil retained in the bionanocomposites after all processing steps. The residual mass of most bionanocomposites was close to or greater than 2 wt% (Table 3), mainly related to the presence of clay in the material. Based on TGA of the clay [21], the clay content in the bionanocomposites was calculated to be between 1.5 and 3 wt% at 500 °C. Because clay acts as a thermal barrier for the volatile products generated during the decomposition, the mass loss tends to be hindered and increases the amount of residue of the samples [26]. Moreover, the residue content was lower in bionanocomposites with G, i.e., PLA/Clay/G, PLA/Clay/10 TT/G, and PLA/Clay/20 TT/G, which may be related to the G improving the dispersion of clay into them and reducing the confinement of organic compounds in montmorillonite galleries. Consequently, such compounds start to interact better with the PLA matrix, reducing the thermal decomposition temperature. This result corroborates the study of Shemesh et al. [27], who evaluated low-density polyethylene bionanocomposites and montmorillonite clay incorporated with carvacrol essential oil and compatibilizer. The latter compound improved the dispersion of the clay-oil hybrid in the polymer matrix, thus reducing the oil content incorporated after processing. However, the antimicrobial activity of the produced films was not compromised immediately; it began to be affected only one month after the preparation of the films.

3.5. Antimicrobial activity on a plastic surface

All experiments met the criteria to be considered valid. First, it was evaluated the ISO221961 requirements for a valid test: L, N, and N24 values. L values were 0.04 and 0.15 for *S. aureus* ATCC 25923 and *E. coli* ATCC25922, respectively. N values were 7.2×10^3 CFU cm^{-2} for *S. aureus* ATCC 25923 and 1.1×10^4 CFU cm^{-2} for *E. coli* ATCC25922. Finally, N24 value of each *S. aureus* replicate was 4.7×10^4, 2.1×10^4, and 2.1×10^4 CFU cm^{-2}, and N24 value of each *E. coli* replicate was 4.1×10^5, 6.3×10^5, and 3.1×10^5 CFU cm^{-2}. All experiments met the ISO 221961 criteria, therefore, were considered valid.

The bionanocomposites' antimicrobial activity was measured based on the ISO221961standard. Table 4 shows the calculated antimicrobial activity (R) obtained for each assay. The data show the essential role of glycerol in film activity, both in gram-positive and gram-negative bacteria. Fig. 5 (a)-(b) shows the results for the bionanocomposites inoculated with *S. aureus* ATCC 25923 and *E.coli* ATCC 25922, respectively, using neat PLA as the control group.

Unexpectedly, a comparison between PLA/Clay bionanocompositeand neat PLA (Fig. 5(a) and (b)) revealed that the presence of clay does not reduce the number of viable cells. According to the literature, clay shows antimicrobial activity even in a low mass percentage [30,31]. This explanation may be related to the hydrophobic character of clay and the polymer matrix that keeps the bacteria adsorbed onto the material surface, reducing the antimicrobial activity of the samples [30]. Hong and Rhim [31] also reported a higher efficiency of clay against gram-positive bacteria, which may be related to the different cellular structures of the microorganisms. According to the authors, gram-positive bacteria show thick cell walls with no outer membrane, whereas gram-negative bacteria have a thin cell wall and an outer membrane. Because the antimicrobial property of clay is related to the organic clay modifier, each type of bacteria reacts differently to the compound. Cloisite® 20A exerts a bacteriostatic effect against gram-positivebacteria, hindering the proliferation of the microorganisms, which justifies the similar number of viable cells in PLA/Clay bionanocomposite and neat PLA.

Among the samples, only PLA/Clay/10 TT/G and PLA/Clay/20 TT/G presented antimicrobial activity against *S. aureus* and *E. coli*, i.e., it was observed antimicrobial activity only in samples with the presence of G. The samples without G (PLA/Clay/10TT and PLA/Clay/20TT) showed no statistically significant reduction compared to the control (pure PLA) and the comparison between these samples without G also has no statistical difference.

The greater clay intercalation/exfoliation observed in the samples with G provided a better diffusion of TT essential oil into the material. On the other hand, regarding PLA/Clay/10TT and PLA/Clay/20TT samples, the poor dispersion of clay into the polymer matrix may have hindered the migration of the oil incorporated into the clay galleries to the material's surface. These results corroborate the transmission electron microscopy images, previously published [15].

Table 4
Antimicrobial activity (R) of the samples against *S. aureus* and *E. coli*.

Sample	Antimicrobial activity (R) (CFU cm^{-2})	
	S. aureus ATCC 25923[a]	*E. coli* ATCC 25922**
PLA/Clay	0.2	−0.1
PLA/Clay/10TT	−0.9	−0.2
PLA/Clay/10 TT/G	3.4	4.6
PLA/Clay/20TT	0.8	0.2
PLA/Clay/20 TT/G	3.4	4.6

[a] U_t of 4.6 CFU cm^{-2} **:U_t of 5.6 CFU cm^{-2}

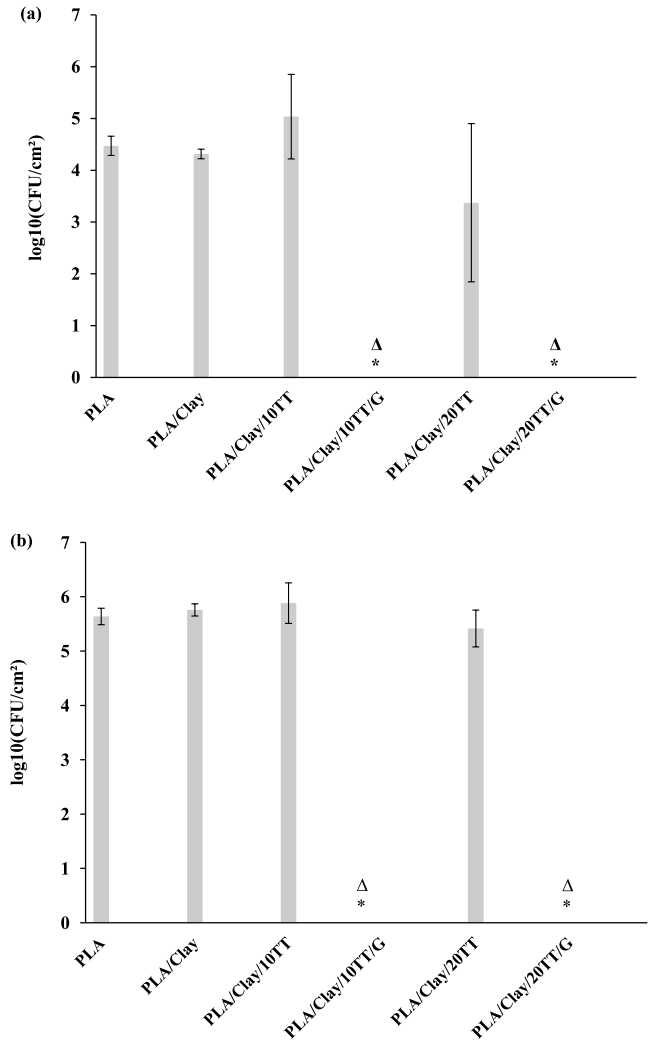

Fig. 5. Reduction in the number of viable cells per cm^2 (CFU cm^{-2}) in PLA, PLA/Clay, PLA/Clay/10TT, PLA/Clay/10 TT/G, PLA/Clay/20TT, and PLA/Clay/20 TT/G extruded bionanocomposites inoculated with (a) *S. aureus* ATCC 25923 and (b) *E. coli* ATCC 25922. Δ: below assay's detection limit; *: $p < 0,05$ - ANOVA test.

The mixture of TT essential oil and G in PLA/Clay/10 TT/G and PLA/Clay/20 TT/G decreased the bacteria population of *S. aureus* and *E.coli* to values below the detection limit of the assay. Again, the presence of G proved interesting for application in antimicrobial wound dressing because it favors the random dispersion of clay lamellas and promotes better permeability of essential oilin the polymeric material. Therefore, the combination of TT essential oil and G is likely to exert a synergistic effect, satisfactorily eliminating gram-positive and gram-negative bacteria and improving the antimicrobial activity of the bionanocomposites.

4. Conclusions

The sonication method used promoted the incorporation of active substances into montmorillonite clay lamellas. Both TT essential oil and glycerol were successfully incorporated into the clay structure as evidenciated by the increase in the interlamellar distance of clay's characteristic $d_{(001)}$ peak. The presence of clay in the bionanocomposites prevents the evaporation of the antimicrobial TT essential oil since it enters the clay galleries due to the interaction with organomodified montmorillonite, as detected by XRD experiments. XRD analyses of the bionanocomposites indicated clay layers were intercalated and exfoliated in the PLA polymer matrix, thus showing the coexistence of both structures. The preparation method efficiently generated a partially exfoliated morphology, contributed by TT essential oil and glycerol, leading to an increase in storage modulus and an up to 10 °C decrease in Tg. However, the TGA results revealed that the bionanocomposites with glycerol addition showed substantial weight loss around the processing temperature, which adversely affects the processing of these materials by melt extrusion. The *in vitro* measurement of antimicrobial activity of the bionanocomposites also revealed that the combination of TT essential oil and glycerol drastically decreased *E.coli* and *S.aureus* viable cells. Although the bionanocomposites studied can be used for antibacterial wound dressing applications, further studies are necessary to evaluate the controlled release of TT oil from the bionanocomposites.

Data availability

The data that supports the findings of this study are available within the article.

CRediT authorship contribution statement

Larissa Braga Proença: Writing – original draft, Methodology, Investigation, Formal analysis, Data curation. **Gabriela Marinho Righetto:** Writing – original draft, Validation, Methodology, Investigation. **Ilana Lopes Baratella da Cunha Camargo:** Writing – review & editing, Project administration, Methodology, Funding acquisition, Data curation. **Marcia Cristina Branciforti:** Writing – review & editing, Writing – original draft, Supervision, Project administration, Methodology, Funding acquisition, Data curation, Conceptualization.

Declaration of competing interest

The authors declare that they have no known competing financial interests or personal relationships that could have appeared to influence the work reported in this paper.

Acknowledgements

The authors acknowledge Coordination of Higher Level Staff Improvement (CAPES) for the financial support, code 001, M.Sc. scholarship (88887.338188/2019–00) of L. B. Proença, Sao Paulo Research Foundation (FAPESP - 2018/15887-4) for the Ph.D scholarship granted to G. M. Righetto, FAPESP and Center for Research and Innovation in Biodiversity and New Drugs (CIBFar-FAPESP grant 2013/07600-3) for the financial support of the antimicrobial tests, and Professor S. P. Campana Filho for the use of the laboratory infrastructure.

References

[1] G.F. Brito, P. Agrawal, E.M. Araújo, T.J.A. Mélo, Rev. Eletron Mater Process 6 (2011) 127–139.
[2] N. Maftoonazad, H. Ramaswamy, Curr. Opin. Food Sci. 23 (2018) 49–56.
[3] S. Gopi, A. Amalraj, Drug Des 5 (2016) 1000129.
[4] Z. Li, M. Knetsch, Curr Pharm Des 24 (2018) 936–951.
[5] C.L. Morelli, M. Mahrous, M.N. Belgacem, M.C. Branciforti, R.E.S. Bretas, J. Bras, Ind. Crops Prod. 70 (2015) 134–141.
[6] F. Tornuk, O. Sagdic, M. Hancer, H. Yetim, Food Res. Int. 107 (2018) 337–345.
[7] M. Alboofetileh, M. Rezaei, H. Hosseini, M. Abdollahi, J. Food Process. Preserv. 42 (2018) e13596.
[8] V. Ojijo, S.S. Ray, Prog. Polym. Sci. 38 (2013) 1543–1589.
[9] T.T. Zhu, C.H. Zhou, F.B. Kabwe, Q.Q. Wu, C.S. Li, J.R. Zhang, Appl. Clay Sci. 169 (2019) 48–66.
[10] E.M.C. Alexandre, R.V. Lourenço, A.M.Q.B. Bittante, I.C.F. Moraes, P.J.A. Sobral, Food Packag Shelf, Life 10 (2016) 87–96.
[11] R.F. Bonan, P.R. F, Bonan, A.U.D. Batista, F.C. Sampaio, A.J.R. Albuquerque, M.C. B. Moraes, L.H.C. Mattoso, G.M. Glenn, E.S. Medeiros, J.E. Oliveira, Mater Sci Eng C 48 (2015) 372–377.
[12] I. Negut, V. Grumezescu, A.M. Grumezescu, Molecules 23 (2018) 2392–2414.
[13] C.F. Carson, S. Messager, K.A. Hammer, T.V. Riley, Aus, Infect Control 10 (2005) 32–34.

[14] F. Solórzano-Santos, M.G. Miranda-Novales, Curr. Opin. Biotechnol. 23 (2012) 136–141.
[15] L.B. Proença, C.A.P. Pena, G.V. Silva, I.L.B.C. Camargo, M.C. Branciforti, Macromol Symp, vol. 394, 2020 2000073.
[16] A.I. Alateyah, H.N. Dhakal, Z.Y. Zhang, Adv. Polym. Technol. 32 (2013) 1–36.
[17] L. Ghaderi, R. Moghimi, A. Aliahmadi, D.J. McClements, H. Rafati, J. Appl. Microbiol. 123 (2017) 832–840.
[18] K.A. Garrido-Miranda, B.L. Rivas, M.A. Pérez-Rivera, E.A. Sanfuentes, C. Peña-Farfal, LWT- Food Sci Technol 98 (2018) 260–267.
[19] B.D. Cullity, Elements of X-Ray Diffraction, Addison-Wesley, London, 1978.
[20] J. Marini, M.C. Branciforti, C. Lotti, Polym. Adv. Technol. 21 (2010) 408–417.
[21] F. Moretti, M.M. Favaro, M.C. Branciforti, R.E.S. Bretas, Polym. Eng. Sci. 50 (2010) 1326–1339.
[22] C.B. Visentini, S.A. Liberman, R.S. Mauler, Polym. Adv. Technol. 26 (2015) 287–293.
[23] S. Molinaro, M. Cruz-Romero, M. Boaro, A. Sensidoni, C. Lagazio, M. Morris, J. Kerry, J. Food Eng. 117 (2013) 113–123.
[24] S. Pavlidou, C.D. Papaspyrides, Prog. Polym. Sci. 33 (2008) 1119–1198.
[25] M.S. Beauvalet, F.F. Mota, R.M.D. Soares, R.V.B. Oliveira, Polym. Bull. 70 (2013) 1863–1873.
[26] V.G.L. Souza, J.R.A. Pires, C. Rodrigues, P.F. Rodrigues, A. Lopes, R.J. Silva, J. Caldeira, M.P. Duarte, F.B. Fernandes, I.M. Coelhoso, A.L. Fernando, Coatings 9 (2019) 700–720.
[27] R. Shemesh, D. Goldman, M. Krepker, Y. Danin-Poleg, Y. Kashi, A. Vaxman, E. Segal, J. Appl. Polym. Sci. 132 (2015) 41261.
[28] M.-A. Paul, M. Alexandre, P. Degée, C. Henrist, A. Rulmont, P. Dubois, Polymer (Guildf) 44 (2003) 443–450.
[29] A. Giannakas, I. Tsagkalias, D.S. Achilias, A. Ladavos, Appl. Clay Sci. 146 (2017) 362–370.
[30] J.-W. Rhim, S.-I. Hong, C.-S. Ha, Food Sci Technol 42 (2009) 612–617.
[31] S.-I. Hong, J.-W. Rhim, J. Nanosci. Nanotechnol. 8 (2008) 5818–5824.